

Effect of weight bearing on recovery from nerve injury in skeletal muscle

TETSUYA MATSUURA,¹ TAKAAKI IKATA,¹ SHINJIRO TAKATA,¹ SHINJI KASHIWAGUCHI,¹ MINEO NIWA,² TAKAYUKI SOGABE,³ AND KEIKO KOGA³

¹Department of Orthopedic Surgery, School of Medicine, University of Tokushima, Tokushima 770-8503;

²Institute for Medicinal Resources, University of Tokushima, Tokushima 770-8505; and

³Tokushima Research Institute, Otsuka Pharmaceutical, Tokushima 771-0192, Japan

Received 19 January 2000; accepted in final form 24 July 2001

Matsuura, Tetsuya, Takaaki Ikata, Shinjiro Takata, Shinji Kashiwaguchi, Mineo Niwa, Takayuki Sogabe, and Keiko Koga. Effect of weight bearing on recovery from nerve injury in skeletal muscle. *J Appl Physiol* 91: 2334–2341, 2001.—We examined the effect of weight bearing (WB) on muscle recovery after nerve injury. Rats were housed in individual cages for 2 wk under WB or hindlimb suspension (HS) after being subjected to sciatic nerve compression for 1 wk. Sham operated on rats served as controls (sham group). We used ³¹P- and ¹⁹F-nuclear magnetic resonance spectroscopy combined with histochemical, physiological, and biochemical techniques to assess the outcome in the three groups. Creatine kinase-BB (CK-BB) mRNA levels expression, CK activity, and type I fiber density in the WB group were elevated compared with those in the HS group. In addition, sciatic functional index, tetanic tension, energy state, and local circulation dynamics of the WB group were greater than those of the HS group. These results suggested that WB plays an important role in muscle regeneration, inhibits the reduction of CK activity, and facilitates the activation of neural recovery, energy state, and local circulation dynamics.

weight bearing; sciatic nerve compression; energy state

DISUSE ATROPHY AFTER IMMOBILIZATION is induced by peripheral nerve injury and has significant physiological and biochemical effects on skeletal muscles, including lost muscle mass, reduced mitochondrial concentration, altered muscle fiber type densities (9), increased resting blood flow (13), altered metabolite levels (13, 15), and decreased resistance to fatigue (13, 15). In response to this injury, skeletal muscles regenerate by activating satellite cells (5), and the changes induced by peripheral nerve injury may reverse themselves. Such a regeneration process is influenced by numerous physiological regulatory factors, including weight bearing (WB), neural activity, and hormones (5, 10, 29). However, little is known about the role of WB during the regeneration of muscles, except that WB can induce synthesis of the slow myosin heavy chain (5). To clarify the role of WB, we have examined its effect on

energy metabolism recovery in an animal model of nerve injury.

The goal of this study was to clarify the effect of WB on the regeneration of muscles with the use of ³¹P- and ¹⁹F-nuclear magnetic resonance (NMR) spectroscopy measurements and more conventional histochemical and physiological methods to assess skeletal muscle recovery in the rat sciatic nerve injury model. In particular, we focused on the gastrocnemius muscle in this study because our preliminary study showed that the gastrocnemius muscle contained >75% of hindlimb muscle mass, and changes in energy states and blood volume monitored by ³¹P- and ¹⁹F-NMR mainly reflected alterations in the gastrocnemius.

METHODS

Animal model. Eighty-one male Sprague-Dawley rats (age = 14 wk) were obtained from SLC Japan and housed in a room with a controlled temperature (25°C) and a 12:12-h light-dark cycle and allowed free access to food and water until the experiments. Muscle degeneration was induced in 68 rats by sciatic nerve compression. Briefly, the right sciatic nerve was exposed through a gluteal muscle-splitting incision and was compressed by placing the nerve trunk within a 1-cm-long silicone tube (0.8-mm internal diameter) under pentobarbital anesthesia (50 mg/kg ip) (22). Three 7-0 nylon sutures were then used to reconstitute the tubing. No surgery was performed on the left side. The silicon tubes were removed after a similar surgical approach 1 wk later. Thereafter, rats were randomly assigned to one of two groups: normal WB ($n = 34$) and hindlimb suspension (HS, $n = 34$). In each group, 3 rats were used to measure tetanic tension, 6 rats were used for ³¹P-NMR, 6 rats were used for histochemical analyses, 12 rats were used for biochemical assays, 1 rat was used for RT-PCR, and 6 rats were used for ¹⁹F-NMR. HS technique used was a modification of the one described by Wronski and Morey-Holton (31). Hindlimbs of animals were raised by using a strip of orthopedic tape attached to the proximal two-thirds of the tail. Suspension height was adjusted to prevent the hindlimbs from contacting the floor or the sides of the cage, while the forelimbs were allowed to support their weight and thus permitted them access to food

Address for reprint requests and other correspondence: T. Matsuura, Dept. of Orthopedic Surgery, School of Medicine, Univ. of Tokushima, 3-18-15, Kuramotocho, Tokushima 770-8503, Japan (E-mail: elbow@clin.med.tokushima-u.ac.jp).

The costs of publication of this article were defrayed in part by the payment of page charges. The article must therefore be hereby marked "advertisement" in accordance with 18 U.S.C. Section 1734 solely to indicate this fact.

and water ad libitum. The remaining 13 rats were evaluated 3 wk after a sham operation and served as the control (sham group). In the sham group, 6 rats were used for histochemical analyses, 6 rats for biochemical assays, and 1 rat for RT-PCR.

Functional assessment. Neural function was assessed from the prints of the hind feet of walking rats by using the sciatic functional index (SFI) described by Medinaceli et al. (24). SFI depends on four factors: distance to opposite foot (TOF), print length (PL), total spreading (TS), and distance between intermediary toes (IT). These variables were measured on both sides and entered in the formula

$$\text{SFI} = [(\text{ETOF} - \text{NTOF})/\text{NTOF} + (\text{NPL} - \text{EPL})/\text{EPL} + (\text{ETS} - \text{NTS})/\text{NTS} + (\text{EIT} - \text{NIT})/\text{NIT}] \times 220/4$$

where E is experimental and N is normal. By using SFI, a value of zero represents normal function and a value of -100% represents complete loss of sciatic nerve function. Bromophenol blue paper and water were used for printing. Neural function was assessed in each rat after 3 and 7 days of sciatic nerve compression and then at 1 and 2 wk after nerve decompression in the WB group and at 2 wk after nerve decompression in the HS group.

Muscle stimulation procedure. Two weeks after nerve decompression, rats were anesthetized by intraperitoneal injection of pentobarbital sodium (50 mg/kg body wt) and placed in the prone position. Two oval electrodes (~4 mm in diameter) were then fixed on the skin of their right legs. Leg muscles were stimulated electrically (SEN-3301, Nihon Kohden, Tokyo, Japan) through an electrode with 0.5-ms square wave pulses of 5 V for 20 min. Stimulation frequency was 40 Hz, which induced a tetanic contraction for a duration of 1 s every 2 s. This frequency continuously produced a minimal tetanic tension. This stimulation procedure was applied to measure tetanic tension, ^{31}P -NMR, and ^{19}F -NMR because, in the preliminary experiments with pulses >5 V (10 V) or frequencies >40 Hz (67 and 100 Hz), differences between WB and HS groups could not be shown because of a significant decrease in signals of high-energy phosphates.

Measurement of tetanic tension. The tendon of the gastrocnemius muscle was exposed at the ankle and then cut and attached to a strain gauge (TB 611, Nihon Kohden) with a noncompliant thread. The strain gauge was connected to a polygraph system (RM-600, Nihon Kohden).

^{31}P -NMR measurement. The right leg of the animal was inserted into a solenoid coil of 2 cm in diameter to record ^{31}P -NMR spectra. Spectra were recorded with a BEM-250/80 NMR instrument (Otsuka Electronics, Osaka, Japan) equipped with a horizontal 250-mm diameter bore magnet (1.9 T). ^{31}P -NMR spectra were obtained at 32.3 MHz with a pulse width of 19 μs (90° pulse). Each spectrum was obtained by 60 scans with a pulse-repetition time of 2 s.

Tissue levels of phosphocreatine (PCr), inorganic phosphate (P_i), and β -ATP were estimated from the areas under individual signals. The energy states were evaluated by the ratio formulas of $\text{PCr}(t)/\text{PCr}(0)$, $\text{PCr}/\beta\text{-ATP}$, and $\text{PCr}/(\text{P}_i + \text{PCr})$, where t means any time of measurement. $\text{PCr}/\beta\text{-ATP}$ measures reliance on PCr stores to maintain ATP levels (27). $\text{PCr}/(\text{P}_i + \text{PCr})$ is related directly to the phosphate potential and can be used as a measure of the muscle bioenergetic reserve and oxidative metabolism (17). Intracellular pH was calculated from the chemical shift (d) of the P_i signal from that of PCr by using the following equation (14)

$$\text{Intracellular pH} = 6.90 - \log[(d - 5.80)/(3.29 - d)]$$

Histological stains. After the silicon tube was removed, the sciatic nerve at the lesion site was prepared for histological

staining. Axon pattern was revealed by hematoxylin and eosin stain, and myelin pattern was demonstrated by a myelin stain. For anti-myelin basic protein (MBP) staining, the sections were immersed in 99% methanol-1% hydrogen peroxide, then blocked with 5% bovine serum albumin (BSA), and incubated with a 1:500 MBP dilution of the antibody in 5% BSA. After that, the sections were washed three times with PBS and then incubated for 2 h with a biotinylated anti-rabbit antiserum (Vector). Staining patterns were revealed with the ABC method (Vector ABC kit), according to the manufacturer's instructions, by using diaminobenzidine as the chromogen.

Histochemical analysis. Rats were killed at the indicated time points, and a 5- to 10-mm cross section was taken from the deep portion of the gastrocnemius muscle. Specimens were immersed in isopentane cooled with liquid nitrogen at -160°C, cut into ~10- μm -thick serial transverse sections with a cryostat (Tissue, TEK II) at -20°C, and stained according to the method of Dubowitz and Brooke (11) with a slight modification of pH and incubation temperature. On the basis of the stainability either with or without acid preincubation at pH 4.2 and 4.3 or 4.4, the muscle fibers of each stage were classified into type I, type IIa, type IIb, and type IIC according to the method of Dubowitz and Brooke (11).

Biochemical assays. Minced gastrocnemius muscles were homogenized in 4 volumes of 10 mM Tris·HCl buffer, pH 7.2, containing 1-mM EDTA in a Polytron homogenizer for 1 min. The homogenate was centrifuged at 10,000 rpm for 20 min. All these procedures were performed at 4°C.

Creatine kinase (CK) activity was determined spectrophotometrically at 30°C in a 5- μl supernatant sample, which was diluted to a final concentration with the same extraction buffer (creatine phosphate kit, CPK-test, WAKO).

Adenylate kinase (AK) activity in the supernatant was measured spectrophotometrically at 340 nm in 50 mM Tris·HCl buffer, pH 7.5, containing (in mM) 5 MgSO₄, 10 glucose, 0.35 NADPH⁺, and 2.5 ADP and a hexokinase and glucose-6-phosphate dehydrogenase-coupled enzyme system by the method of Colowick and Kaplan (8) with a slight modification.

Protein concentration was determined by the method of Bradford (6). All spectrophotometric measurements were made by using a Hitachi spectrophotometer, model 624.

RT-PCR. Three isozymes (MM, MB, and BB) of CK (1) and three isozymes (AK1, AK2, and AK3) of AK (28) have been characterized to date. RT-PCR was used to measure mRNA levels of CK-MM, the major cytosolic isoform found in muscles; CK-BB, the embryonic isoform found in muscles; and AK-3. Total RNA was extracted from the gastrocnemius muscle by the acid-guanidinium isothiocyanate phenol chloroform (AGPC) method (7). RT-PCR was performed according to a modification of the method described by Liu et al. (20). Briefly, the first strand cDNA was synthesized by using an oligo(dT) 15 primer (Seikagaku) and M-MLV reverse transcriptase (USB) followed by PCR amplification using synthetic gene specific primers for rat CK-MM, CK-BB, AK-3, or G3PDH. Oligonucleotide primers used were 5'-CAGAGCAGGATCAACAACGGC-3' (sense) and 5'-TTGATGTCCTGGCCTCTCTCC-3' (anti-sense) for rat CK-MM (2); 5'-GACGACCACTTCTCTTCGAC-3' (sense) and 5'-CTTCTCGTGCTTTC-CAGGTG-3' (anti-sense) for rat CK-BB (3); 5'-CGATGACCTAACGGGAGAACC-3' (sense) and 5'-CTGAGCTAAATC-CCCAACCCC-3' (anti-sense) for rat AK-3 (28); and 5'-TCCCTCAAGATTGTGACGAA-3' (sense) and 5'-AGATCCACAACGGATACATT-3' (anti-sense) for rat glyceraldehyde-3-phosphate dehydrogenase (GAPDH) (20). PCR amplification was performed according to the standard methods using *Taq* polymer-

ase (Promega, Madison, WI). After initial denaturation for 4 min at 94°C, 30 cycles of amplification (95°C for 1 min, 55°C for 1 min, and 72°C for 4 min) were followed by a 10-min extension at 72°C by using a program temperature control system PC700 (ASTEC, Tokyo, Japan). Possible contamination with PCR components was excluded by performing PCR with these components in the absence of the RT product in each set of experiments (negative control). PCR products were separated in 2% agarose gels, which contained ethidium bromide and visualized under ultraviolet light.

¹⁹F-NMR measurement. The right leg of the animal was inserted into a 2-cm-diameter solenoid coil to record ¹⁹F-NMR spectra. Spectra were recorded with a BEM 250/80 NMR instrument (Otsuka Electronics) equipped with a horizontal 250-mm diameter bore magnet (1.9 T). ¹⁹F-NMR spectra were obtained at 75.1 MHz with a pulse width of 45 μs (90° pulse). Each spectrum was obtained by 60 scans with a pulse-repetition time of 2 s. For the ¹⁹F-NMR study, FC-43 emulsion, an emulsion of 20% wt/vol perfluorotributylamine (FC-43; Green Cross), was injected via the femoral vein (5 ml/kg body wt) as an intravascular tracer. FC-43 has four ¹⁹F signals that have been assigned (CF₃, CF₂, CF₂, and CF₂), of which the CF₃ signal has been found to be more sensitive than the three CF₂ signals. Local circulation dynamics were evaluated by the ratio formula of CF₃(t)/CF₃(0).

Measurement of muscle wet weight. At the end of the experiments, the gastrocnemius muscle on the right side was removed, cleaned of connective tissue, and weighed. Degree of atrophy was determined in the two groups.

Statistical analysis. All values are presented as means ± SD. Data of functional assessment (SFI), maximum tetanic tension, muscle weight, density of muscle fibers, and the data of ³¹P- and ¹⁹F-NMR at rest were analyzed by using Student's *t*-test. The data of ³¹P- and ¹⁹F-NMR during and after stimulation were analyzed by using a three-way ANOVA to assess the significance of differences related to group or time. A *P* value of <0.05 was regarded as significant.

RESULTS

SFI. SFI at the end of the experiment and time course of changes are shown in Table 1 and Fig. 1, respectively. SFI decreased to about -100% within three days of compression of the sciatic nerve. In the WB group, recovery of SFI was apparent 1 wk after decompression and improved significantly to about -70% in 2 wk, whereas, in the HS group, SFI remained at about -100% during the experiment. These results indicate that WB seems to facilitate recovery of neural function.

Histological stains. After 1 wk of nerve compression, histological examination revealed swelling and decom-

Table 1. BW, MW, and SFI

	WB Group (n = 34)	HS Group (n = 34)
BW, g	426 ± 16*	356 ± 21
MW, g	0.83 ± 0.11*	0.67 ± 0.05
MW/BW × 10 ³	2.01 ± 0.03*	1.78 ± 0.03
SFI, %	-72 ± 18*	-120 ± 13

Values are means ± SD. BW, body weight; MW, muscle weight; SFI, sciatic function index; WB, weight bearing; HS, hindlimb suspension. Values of the WB group were compared with those of the HS group. *Significant difference (*P* < 0.05).

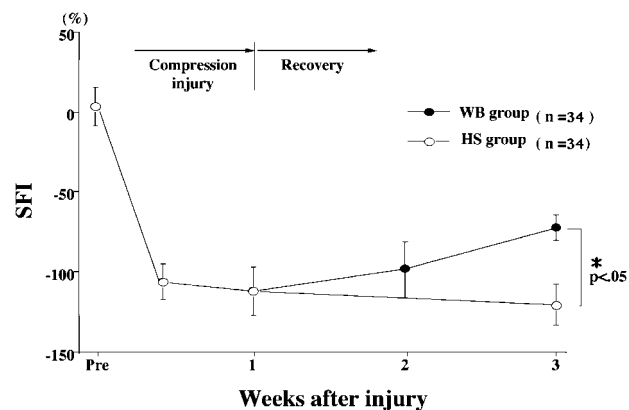


Fig. 1. Time course of changes of the sciatic functional index (SFI) in rats subjected to compression injury of the sciatic nerve. In the weight bearing (WB) and hindlimb suspension (HS) groups, the silicone tubes that compressed the sciatic nerves were removed after 1 wk.

position of the axons and expansion and deformity of myelin.

Wet muscle weight. Gastrocnemius muscle weights in the WB and HS groups are shown in Table 1. Absolute and relative muscle weights were significantly higher in the WB group than in the HS group (*P* < 0.05).

Tetanic tension. Maximum tension at 40 Hz was 95 ± 12 g in the WB group and 58 ± 12 g in the HS group. Tension per gram of muscle was 116 ± 9 g in the WB group and 88 ± 11 g in the HS group. WB resulted in significantly higher tension (*P* < 0.05).

Muscle energy state and intracellular pH. Time course of changes in PCr(t)-to-PCr(0) and PCr-to-β-ATP ratios is shown in Figs. 2 and 3, respectively. PCr(t)-to-PCr(0) ratios of the WB and HS groups showed minimal values of 0.68 ± 0.10 and 0.63 ± 0.08, respectively, at 2 min after the onset of electrical stimulation. In both groups, PCr(t)-to-PCr(0) ratio subse-

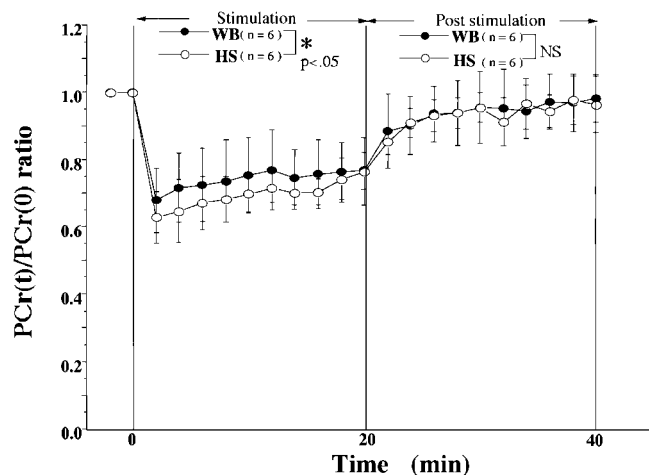


Fig. 2. Time course of changes in PCr(t)-to-PCr(0) ratio during and after stimulation. During stimulation, the ratio was significantly higher in the WB group compared with the HS group (*P* < 0.05). Values are means ± SD. PCr, phosphocreatine; *t*, any time of measurement; NS, not significant.

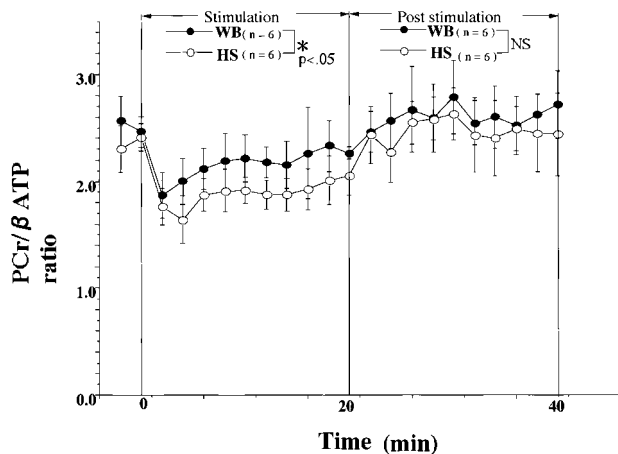


Fig. 3. Time course of changes in PCr-to- β -ATP ratio before, during, and after stimulation. During stimulation, the ratio was significantly higher in the WB group compared with the HS group ($P < 0.05$). Values are means \pm SD.

quently increased with time, but it was significantly higher in the WB group than in the HS group during stimulation ($P < 0.05$). In the poststimulation stage, PCr(t)-to-PCr(0) ratio gradually returned to initial values in both groups without showing a significant difference between them. PCr-to- β -ATP ratio of the WB group demonstrated a minimal value of 1.87 ± 0.21 at 2 min after the start of electrical stimulation in contrast with a minimal value of 1.64 ± 0.23 in the HS group at 4 min after the start of the electrical stimulation. In both groups, PCr-to- β -ATP ratio subsequently increased with time and remained significantly higher in the WB group than in the HS group during stimulation ($P < 0.05$). In the poststimulation stage, PCr-to- β -ATP ratio gradually returned to initial values in both groups without showing a significant difference between them.

Time course of changes in PCr/($P_i + PCr$) ratio is shown in Fig. 4. PCr/($P_i + PCr$) of the WB group

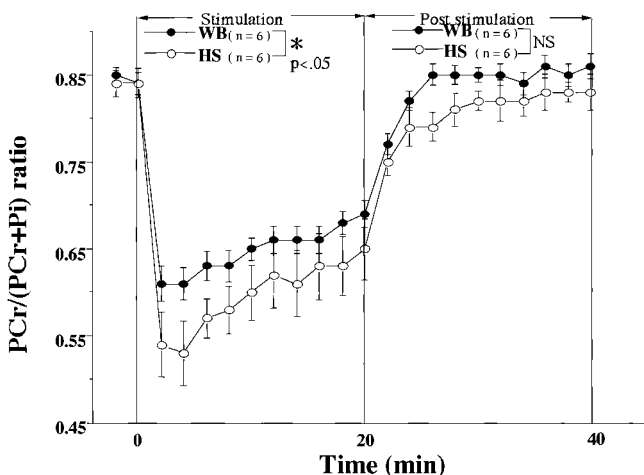


Fig. 4. Time course of changes in PCr-to-($P_i + PCr$) ratio before, during, and after stimulation. During stimulation, the ratio was significantly higher in the WB group compared with the HS group ($P < 0.05$). Values are means \pm SD. P_i , inorganic phosphate.

demonstrated a minimal value of 0.61 ± 0.02 at 2 min after the start of electrical stimulation compared with a minimal value of 0.53 ± 0.04 in the HS group at 4 min after the start of electrical stimulation. In both groups, PCr/($P_i + PCr$) subsequently increased with time and remained significantly higher in the WB group than in the HS group during stimulation ($P < 0.05$). In the poststimulation stage, PCr/($P_i + PCr$) gradually returned to initial values in both groups.

Changes in intracellular pH are illustrated in Fig. 5. After the start of stimulation, pH decreased and reached its lowest level within 4 min (6.6 ± 0.2 in the WB group and 6.6 ± 0.2 in the HS group). From minute 4 to the end of stimulation, intracellular pH gradually increased and returned to the resting value. There was no significant difference in intracellular pH between the two groups throughout the experiment.

Histochemical analysis. Figure 6 shows muscular fiber-type differentiation as revealed by ATPase activities in the gastrocnemius muscle of the sham, WB, and HS groups. As shown in Table 2, the gastrocnemius muscle of the HS group contained a lower percentage of type I and IIa fibers but a higher percentage of type IIb and IIc fibers than the sham group ($P < 0.05$), whereas the gastrocnemius muscle of the WB group had a higher percentage of type I and type IIa fibers but a lower percentage of type IIb fibers than the HS group ($P < 0.05$).

Biochemical assays. We measured CK and AK activity after all samples were homogenized together in each group because the minced gastrocnemius muscles of the WB and HS groups were so small that we could not measure individual samples. So we did not perform the statistical analysis. As shown in Table 3, CK activity was 2.5 times higher in the WB group than in the HS group, but no difference was found regarding AK activities between the WB and HS groups.

RT-PCR. CK and AK mRNA expression in the gastrocnemius muscle of the sham, WB, and HS groups was investigated. PCR products amplified by using G3P DH-, CK-MM-, CK-BB-, and AK-3-specific primers showed clear bands of the predicted sizes (Fig. 7).

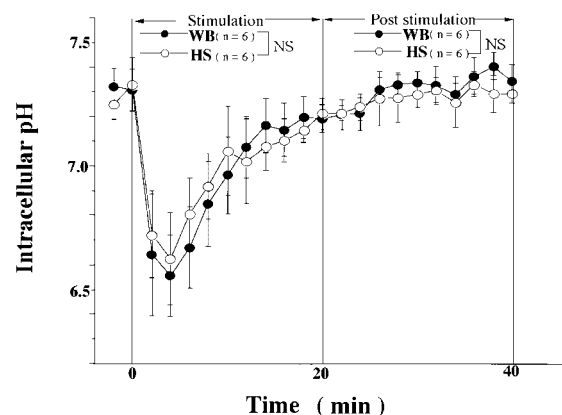


Fig. 5. Time course of changes in intracellular pH before, during, and after stimulation. No significant differences were observed between WB and HS groups. Values are means \pm SD.

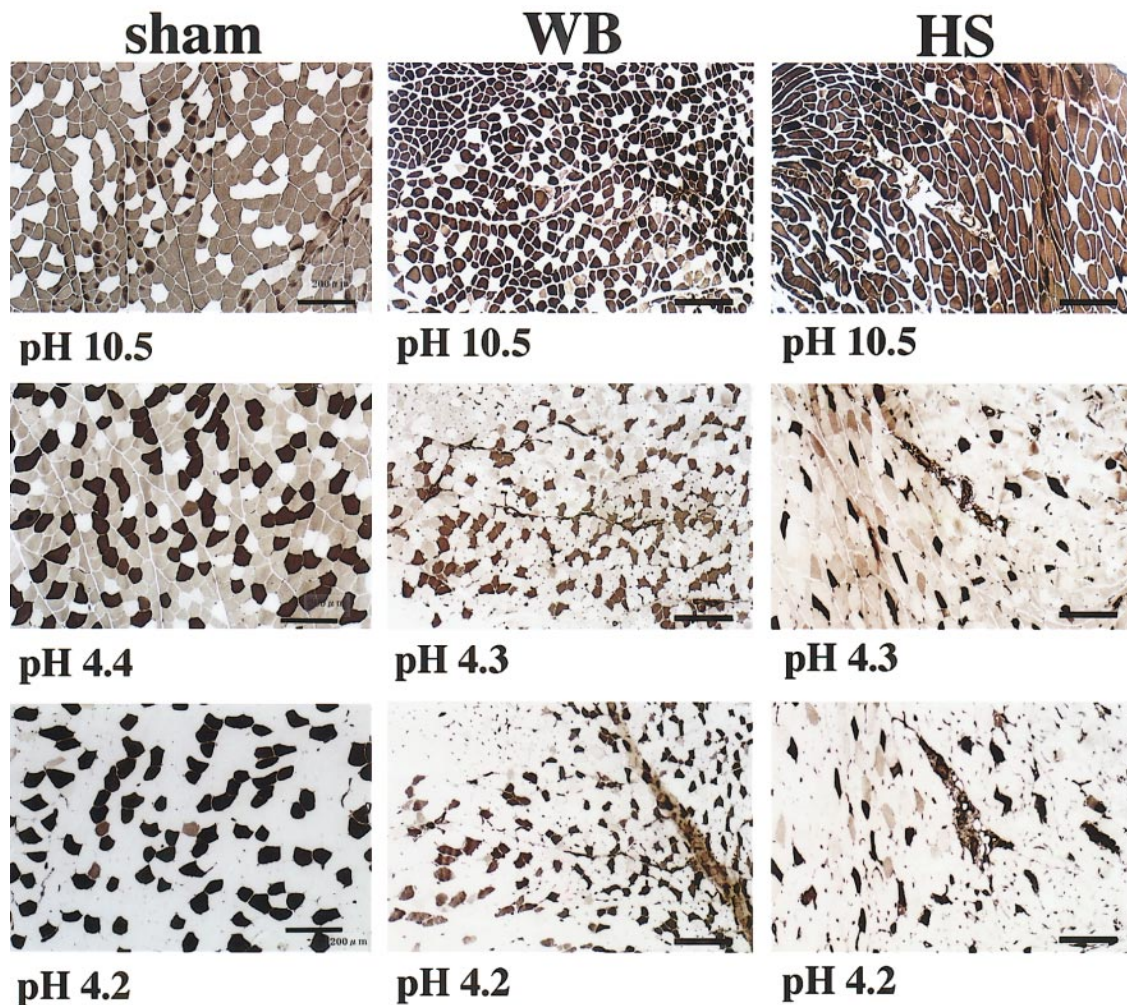


Fig. 6. Fiber type differentiations as revealed by ATPase activities in the gastrocnemius muscle of sham, WB, and HS groups. Fibers stained at pH 10.5. Adjacent sections were preincubated at pH 4.4 or 4.3 and 4.2, respectively. Calibration bar = 200 μm .

Expression of CK-MM mRNA in the WB and HS groups was reduced compared with the sham group, and no difference was found in the expression of CK-MM mRNA between the WB and HS groups. On the other hand, whereas no appreciable CK-BB signal was detected in the sham group, this signal was clearly detected in the WB and HS groups. In the WB group, the expression of CK-BB mRNA was increased compared with the HS group. In the WB group, however, expression of AK-3 mRNA was reduced compared with the HS group.

Table 2. *Histochemical data*

Group	Type I	Type IIa	Type IIb	Type IIc (%)
Sham (<i>n</i> = 6)	26.0 \pm 3.2	14.5 \pm 0.5	58.8 \pm 4.2	0.7 \pm 0.2
WB (<i>n</i> = 6)	23.0 \pm 5.5*	14.3 \pm 0.8*	59.6 \pm 2.6*	3.1 \pm 0.6
HS (<i>n</i> = 6)	9.1 \pm 0.5	10.1 \pm 0.5	77.6 \pm 5.5	3.2 \pm 0.5

Values are means \pm SD. Values of the WB group were compared with those of the HS group. *Significant difference ($P < 0.05$).

Muscle circulation dynamics. Time course of changes in $CF_3(t)/CF_3(0)$ is shown in Fig. 8. $CF_3(t)$ -to- $CF_3(0)$ ratios of the WB group and HS groups increased to a maximum of 115 ± 15 and 110 ± 12 , respectively. During stimulation, $CF_3(t)/CF_3(0)$ was significantly higher in the WB group than that in the HS group ($P < 0.05$). In the poststimulation stage, $CF_3(t)/CF_3(0)$ decreased to the prestimulation value in the HS group, whereas, in the WB group, the value decreased but did not reach the prestimulation value.

Table 3. *Enzyme activity*

Group	AK, nmol NADPH produced \cdot min ⁻¹ \cdot mg protein ⁻¹	CK, nmol NBT reduced \cdot min ⁻¹ \cdot mg protein ⁻¹
Sham (<i>n</i> = 6)	419 \pm 17	1.21 \pm 0.02
WB (<i>n</i> = 12)	350 \pm 4	0.63 \pm 0.04
HS (<i>n</i> = 12)	422 \pm 22	0.25 \pm 0.01

Values are the means \pm SD. AK, adenylate kinase; CK, creatine kinase.

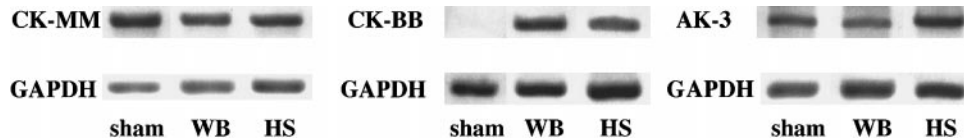


Fig. 7. PCR products amplified by using glyceraldehyde-3-phosphate dehydrogenase (GAPDH)-, CK-MM-, CK-BB-, and AK-3-specific primers. No difference was found in the expression of CK-MM mRNA in each muscle between WB and HS groups. However, in the WB group, expression of CK-BB mRNA signal was increased compared with the HS group, whereas, in the WB group, the expression of AK-3 mRNA was reduced compared with the HS group.

DISCUSSION

Peripheral nerve injuries involving axonal interruption can be subdivided into those in which the continuity of the nerve is preserved and those in which the nerve is severed (13). In this study, we used a nerve compression model that belongs to the former. Previous studies have shown changes in the expression of myosin isoforms (5), enzyme activities (26), energy states, and blood volume (16) in denervated muscles during regeneration. The regeneration process is affected by WB. Bigard et al. (5) showed the influence of WB on the expression of myosin isoform during regeneration. In this study, we examined the effect of WB on histochemical changes, energy states, activities, and gene expressions of both CK and AK, and blood volume during regeneration in an animal model of nerve injury.

Histochemical analysis revealed that the percentage of type I fibers in the gastrocnemius muscle of the WB group was higher than that of the HS group (Table 2). Because the percentage of type I fibers of the sham group was similar to that of the WB group, these results suggested that WB inhibited the decrease in type I fiber density during the regeneration process. In addition, the gastrocnemius muscle of the WB group contained a higher percentage of type IIa fibers than that of the HS group (Table 2). Endurance training also increases the number of highly oxidative (type IIa) fibers at the expense of the glycolytic IIb fibers (21).

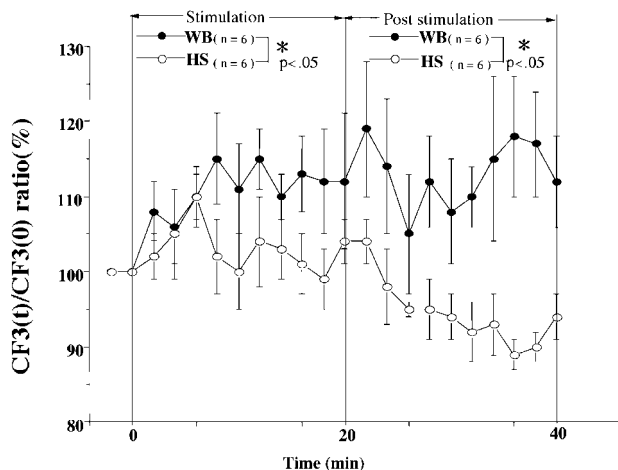


Fig. 8. Time course of changes in $CF_3(t)$ -to- $CF_3(0)$ ratio before, during, and after stimulation. During and after stimulation, the ratio was significantly greater in the WB group compared with the HS group ($P < 0.05$). Values are means \pm SD.

These data suggest that WB induced a type IIb-to-type IIa fiber transformation during the regeneration process.

We selected a stimulation pulse frequency of 40 Hz and a voltage of 5 V because, under these conditions, a suitable tetanic contraction was induced in the WB group. During tetanic contraction induced by 40 Hz, $PCr(t)/PCr(0)$, PCr/β -ATP, and $PCr/(P_i + PCr)$ were significantly higher in the WB group than in the HS group (Figs. 2–4). These observations suggested that the WB group kept a higher phosphate potential to maintain ATP levels. Previous ^{31}P -NMR studies using a unilateral sciatic nerve injury model showed that the energy states of denervated skeletal muscles returned to normal with neural recovery (16), and the present study demonstrated that WB facilitated the recovery of the energy states during the regeneration process. Bessman and Carpenter (4) reported that, as for ATP production, there are the following energy states: 1) $PCr + ADP \rightarrow creatine + ATP$ and 2) $2ADP \rightarrow ATP + AMP$.

Our data showed that there was a significantly higher level of CK activity in the gastrocnemius muscle of the WB group than in that of the HS group, although there was no difference in AK activity of the gastrocnemius muscle in either group (Table 3). This finding suggests that the significantly higher muscle energy state in the WB group, compared with the HS group, during contraction was because of the significantly higher level of CK activity in the gastrocnemius muscle of the WB group.

There are three major forms of CK (CK-MM, CK-MB, and CK-BB) in mammals. In skeletal muscles, a switch of CK isoenzymes from predominance of embryonic BB isoenzyme to MM isoenzymes occurs during development (1). Our data demonstrated that the expression of CK-MM mRNA in the WB and HS groups was reduced compared with that in the sham group, and a CK-BB signal was detected in the WB and HS groups, although no appreciable signal was detected in the sham group. The level of CK-BB mRNA expression in the gastrocnemius muscle was greater in the WB group than in the HS group, but no difference was found in the expression of CK-MM (Fig. 7). In adult muscles of mammals, regeneration generally reproduces many of the events that characterize normal development (5). The present findings indicated that WB facilitated the recovery of CK gene expression during the regeneration process. Recently, transgenic mice that express the B subunit of CK in skeletal muscle have been

described (25) and reported to show increased total CK activity. Our results demonstrated that the increased expression of CK-BB mRNA in the WB group was partly responsible for the increased CK activity in this group compared with the HS group. On the other hand, three AK isoenzymes (AK-1, AK-2, and AK-3) have been characterized. AK-3 mRNA was detected in most tissues, indicating that AK-3 gene expression is constitutive. AK-3 mRNA was shown to be present at high levels during the fetal stage and to remain fairly constant during development (28). Expression of AK-3 mRNA in the WB group was reduced compared with the HS group (Fig. 8), suggesting that WB induced a decrease of AK-3 mRNA in contrast to CK-BB mRNA expression, which was higher in the WB group than in the HS group. This finding was consistent with the hypothesis that a marked increase of AK-catalyzed phosphotransfer occurs when CK catalytic velocity is suppressed in skeletal muscles (12, 32).

In addition, with regard to the local circulation dynamics, muscle blood volume in the WB group was higher than in the HS group during and after contraction (Fig. 8). Our results showed that peripheral vessels in the WB group were more capable of vasodilation during contraction for keeping a high sensitivity to vasodilator substance after WB than in the HS group. These facts suggested that WB stimulated peripheral vessels and contributed to maintain their ability to vasodilate during the regeneration process. Furthermore, in our previous study, it was shown that the recovery of circulation preceded that of the energy state in skeletal muscles (16); thus the higher increase of muscle blood volume observed in the WB group might be the reason for the preservation of ATP levels in this group.

Our results further support the hypothesis that WB plays an important role in muscle regeneration because WB inhibited decreases in type I fiber density and CK activity and facilitated activation of neural function, energy state, and local circulation dynamics.

The authors thank Yasuyuki Tsutsumishita, Tomoaki Onda (Institute for Medicinal Resources, University of Tokushima), Makoto Ishikawa, Junya Kohara, Mari Fukunaga, and Toshiko Nakashima (Tokushima Research Institute, Otsuka Pharmaceutical) for valuable suggestions and assistance in this study.

REFERENCES

1. **Apple FS and Billadello JJ.** Expression of creatine kinase M and B mRNAs in treadmill trained rat skeletal muscle. *Life Sci* 55: 585–592, 1994.
2. **Benfield PA, Graf D, Korolkoff PN, Hobson G, and Pearson ML.** Isolation of four rat creatine kinase genes and identification of multiple potential promoter sequences within the rat brain creatine kinase promoter region. *Gene* 63: 227–243, 1988.
3. **Benfield PA, Henderson L, and Pearson ML.** Expression of a rat brain creatine kinase- β -galactosidase fusion protein in *Escherichia coli* and derivation of the complete amino sequence of rat brain creatine kinase. *Gene* 39: 263–267, 1985.
4. **Bessmann SP and Carpenter CL.** The creatine-creatine phosphate energy shuttle. *Annu Rev Biochem* 54: 831–862, 1985.
5. **Bigard XA, Mario D, Serrurier B, Lienhard F, Guezennec YC, Bockholdt KJ, and Whalen RG.** Role of weight bearing function on expression of myosin isoforms during regeneration of rat soleus muscles. *Am J Physiol Cell Physiol* 270: C763–C771, 1996.
6. **Bradford MM.** A rapid and sensitive method for the quantitation of microgram quantities of protein utilizing the principle of protein-dye binding. *Anal Biochem* 72: 248–254, 1976.
7. **Chomczynski P and Sacchi N.** Single-step method of RNA isolation by acid guanidinium thiocyanate-phenol-chloroform extraction. *Anal Biochem* 162: 156–159, 1987.
8. **Colowick SP and Kaplan NO.** Adenylate kinase. In: *Methods in Enzymology*. New York: Academic, 1955, p. 598–604.
9. **Daemen MA, Kurvers HA, Bullens PH, Slaaf DW, Freling G, Kitslaar PJ, and van den Wildenberg FA.** Motor denervation induces altered muscle fiber type densities and atrophy in a rat model of neuropathic pain. *Neurosci Lett* 247: 204–208, 1998.
10. **D'Albis AM, Lanfant-Guyot CJ, Chanoine C, Weinman J, and Gallien C.** Regulation by thyroid hormones of terminal differentiation in the skeletal dorsal muscle. Neonatal muscle. *Dev Biol* 123: 25–32, 1987.
11. **Dubowitz V and Brooke MH.** *Muscle Biopsy. A Modern Approach*. London: Saunders, 1973.
12. **Dzeja PP, Zeleznikar RJ, and Goldberg ND.** Suppression of creatine kinase-catalyzed phosphotransfer results in increased phosphoryl transfer by adenylate kinase in intact skeletal muscle. *J Biol Chem* 271: 12847–12851, 1996.
13. **Eisenberg HA and Hood DA.** Blood flow, mitochondria, and performance in skeletal muscle after denervation and reinnervation. *J Appl Physiol* 76: 859–866, 1994.
14. **Flaherty JT, Weisfeldt MS, Bulkley BH, Gardner TJ, Gott VL, and Jacobus WE.** Mechanism of ischemic myocardial cell damage assessed by phosphorus-31 nuclear magnetic resonance. *Circulation* 65: 561–571, 1982.
15. **Gupta RC, Misulis KE, and Dettbarn WD.** Activity dependent characteristics of fast and slow muscle: biochemical and histochemical considerations. *Neurochem Res* 14: 647–655, 1989.
16. **Hayashi Y, Ikata T, Takai H, Takata S, Sogabe T, and Koga K.** Time course of recovery from nerve injury in skeletal muscle-energy state and local circulation. *J Appl Physiol* 82: 732–737, 1997.
17. **Kemp GJ, Thompson CH, Bernes PRJ, and Radda GK.** Comparisons of ATP turnover in human muscle during ischemic and aerobic exercise using ^{31}P magnetic resonance spectroscopy. *Magn Reson Med* 31: 248–258, 1994.
18. **Laughlin MH and Armstrong RB.** Muscle blood flow during locomotory exercise. *Exerc Sport Sci Rev* 13: 95–136, 1985.
19. **Linderman JK, Kristin LG, Frank WB, Venkat RM, and Richard EG.** Resistance exercise and growth hormone as countermeasures for skeletal muscle atrophy in hindlimb-suspension rats. *Am J Physiol Regulatory Integrative Comp Physiol* 267: R365–R371, 1994.
20. **Liu S, Adcock IM, Old RW, Barnes PJ, and Evans TW.** Lipopolysaccharide treatment in vivo induces widespread tissue expression of inducible nitric oxide synthase mRNA. *Biochem Biophys Res Commun* 196: 1208–1213, 1993.
21. **Mabuchi K, Szvetko D, Pinter K, and Sreter FA.** Type IIb to IIa fiber transformation in intermittently stimulated rabbit muscles. *Am J Physiol Cell Physiol* 242: C373–C381, 1982.
22. **Mackinnon SE, Dellon AL, Hudson AR, and Hunter DA.** Chronic nerve compression—an experimental model in the rat. *Ann Plast Surg* 13: 112–120, 1984.
23. **McDonald KS, Delp MD, and Fitts RH.** Fatigability and blood flow in the rat gastrocnemius-plantaris-soleus after hindlimb suspension. *J Appl Physiol* 73: 1135–1140, 1992.
24. **Medinaceli L, Freed WJ, and Wyatt RJ.** An index of the functional condition of rat sciatic nerve based on measurement made from walking tracks. *Exp Neurol* 77: 634–643, 1982.
25. **Roman BB, Jeanne MF, Ron AM, and Alan PK.** Contractile and metabolic effects of increased creatine kinase activity in mouse skeletal muscle. *Am J Physiol Cell Physiol* 270: C1236–C1245, 1996.

26. **Sesodia S, Choksi RM, Ron AM, and Nemeth PM.** Nerve-dependent recovery of metabolic pathways in regenerating soleus muscles. *J Muscle Res Cell Motil* 15: 573–581, 1994.
27. **Spurway NC and Wray S.** A phosphorus nuclear magnetic resonance study of metabolites and intracellular pH in rabbit vascular smooth muscle. *J Physiol (Lond)* 393: 57–71, 1987.
28. **Tanabe T, Yamada M, Noda T, Kajii T, and Nakazawa A.** Tissue-specific and developmentally regulated expression of the genes encoding adenylate kinase isozymes. *J Biochem (Tokyo)* 113: 200–207, 1993.
29. **Whalen RG, Harris JB, Butler-Browne GS, and Sesodia S.** Expression of myosin isoforms during notexin-induced regeneration of rat soleus muscles. *Dev Biol* 141: 24–40, 1990.
30. **Wicks KL and Hood DA.** Mitochondrial adaptations in denervated muscle. *Am J Physiol Cell Physiol* 260: C841–C850, 1991.
31. **Wronski TJ and Morey-Holton ER.** Skeletal response to stimulated weightlessness: a comparison of suspension techniques. *Aviat Space Environ Med* 58: 63–68, 1987.
32. **Zelevnikar RJ, Dzeja PP, and Goldberg ND.** Adenylate kinase-catalyzed phosphoryl transfer couples ATP utilization with its generation by glycolysis in intact muscle. *J Biol Chem* 271: 7311–7319, 1995.
33. **Zochodne DW, Thompson RT, Driedger AA, Strong MJ, Gravelle D, and Bolton CF.** Metabolic changes in human muscle denervation: topical ^{31}P -NMR spectroscopy studies. *Magn Reson Med* 7: 373–383, 1988.

